IEICE TRANS. ELECTRON., VOL.E99–C, NO.7 JULY 2016

PAPER Special Section on Recent Advances in Simulation Techniques and Their Applications for Electronics

A Study on Single Polarization Guidance in Photonic Band Gap Fiber with Anisotropic Lattice of Circular Air Holes

Kazuki ICHIKAWA[†a)], **Zejun ZHANG**[†b)], ***Student Members***, **Yasuhide TSUJI**[†c)], ***and*** **Masashi EGUCHI**[††d)], ***Members***

SUMMARY We propose a novel single polarization photonic band gap fiber (SP-PBGF) with an anisotropic air hole lattice in the core. An SP-PBGF with an elliptical air hole lattice in the core recently proposed can easily realize SP guidance utilizing the large difference of cutoff frequency for the *x*- and *y*-polarized modes. In this paper, in order to achieve SP guidance based on the same principle of this PBGF, we utilize an anisotropic lattice of circular air holes instead of elliptical air holes to ease the fabrication difficulty. After investigating the influence of the structural parameters on SP guidance, it is numerically demonstrated that the designed SP-PBGF has 381 nm SP operating band.

key words: *photonic crystal fiber, Single polarization guidance, photonic band gap, anisotropic air hole lattice, birefringence*

1. Introduction

In the rapid spread of the Internet, the demand for high speed and large capacity optical communication system is increasing. However, conventional fibers are not thought to be adequate and thus a novel high performance optical fiber is desired. Under this circumstance, in order to expand the communication capacity and to achieve high-speed transmission, various new types of high performance optical fibers have been studied. One of these fibers is photonic crystal fibers (PCFs) with interesting features [1]–[4]. These fibers can be generally classified into two types referred to as holey fibers (HFs) and photonic band gap fibers (PBGFs) according to their guidance mechanism.

In recent years, the single polarization (SP) devices utilized in digital coherent communications have been also studied. The ordinary PCFs with a triangular lattice of air holes have a sixfold symmetry and the two orthogonally polarized modes in these fibers are degenerate. Therefore, in order to obtain birefringence, some structural asymmetry has to be introduced into the core or cladding and several types of SP-PCF have been reported [5]–[14]. One of these approaches is to utilize elliptical air holes and the PCF with an elliptical air hole lattice in the core has been reported [12], [13]. In these PCFs, the SP guidance is easy to achieve by using the isotropic effective index of the fundamental space-filling mode (FSM) in the cladding with circular air holes and the anisotropic FSM index in the core with elliptical air holes. However, in general, the elliptical air holes require sophisticated fabrication process. In [14], instead of elliptical air holes, an anisotropic lattice of circular air holes is used to design an SP-HF.

In this paper, we present a novel SP-PBGF with an anisotropic air hole lattice in the core region. Our SP-PBGF with only circular air holes has a simple structure comparing to that with an elliptical air hole lattice. In Sect. 2, we indicate the finited-element methods to calculate the mode field distributions and propagation constant. In Sect. 3, we demonstrate the SP guidance can be achieved in the proposed SP-PBGF. In Sect. 4, we investigate the diameter and lattice pitch dependences of the SP bandwidth in our SP-PBGF. In Sect. 5, we design the SP-PBGF to broaden the SP band and this paper is concluded in Sect. 5.

2. Finite Element Method for Photonic Crystal Fibers

Our proposed single-polarization PBGFs shown in Fig. 1 have a uniform structure in *z* direction and the periodic structure in the *x*-*y* plane, and the light propagates along the *z* direction in this fiber. From Maxwell's equations, we obtain

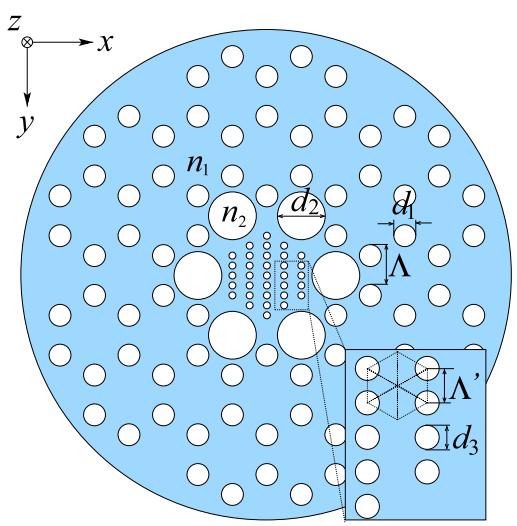

Fig. 1 Cross-section of the proposed SP-PBGF with an anisotropic lattice of circular air holes.

Manuscript received October 20, 2015.
Manuscript revised February 20, 2016.

[†]The authors are with Information and Electronic Eng., Muroran Insitute of Technology, Muroran-shi, 050–8585 Japan
[††]The author is with Department of Opt-Electronic System Eng., Chitose Institute of Science and Technology, Chitose-shi, 066–8655 Japan
a) E-mail: 14043004@mmm.muroran-it.ac.jp
b) E-mail: 12054072@mmm.muroran-it.ac.jp
c) E-mail: y-tsuji@mmm.muroran-it.ac.jp
d) E-mail: megu@ieee.org

DOI: 10.1587/transele.E99.C.774

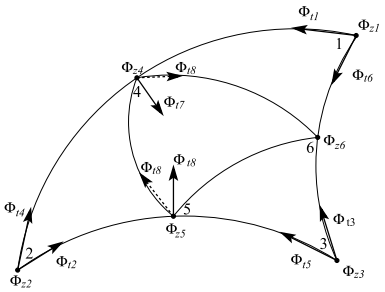

Fig. 2 Curvilinear hybrid edge/nodal element.

the following wave equation,

$$\nabla \times (p\nabla \times \mathbf{\Phi}) - k_0^2 q\mathbf{\Phi} = 0 \tag{1}$$

where μ_r and ε_r are the relative permeability and relative permittivity, respectively, k_0 is the free-space wavenumber, and $\mathbf{\Phi}$ represents either the electric field $\mathbf{E}$ or the magnetic field $\mathbf{H}$ and

$$p = \mu_r^{-1},\ q = \varepsilon_r \quad \text{for} \quad \mathbf{\Phi} = \mathbf{E} \tag{2}$$

$$p = \varepsilon_r^{-1},\ q = \mu_r \quad \text{for} \quad \mathbf{\Phi} = \mathbf{H}. \tag{3}$$

In this paper, the curvilinear edge/nodal hybrid elements [15], as shown in Fig. 2, are employed to discretize the x-y plane. Expressing the field $\mathbf{\Phi}$ as

$$\mathbf{\Phi}(x, y, z) = \boldsymbol{\phi}(x, y)\exp(-j\beta z) \tag{4}$$

and applying the vector finite-element method (FEM) to (1), we obtain the eigenvalue problem,

$$\left([K] - \beta^2[M]\right)\{\phi\} = \{0\} \tag{5}$$

where $[K]$ and $[M]$ are the finite-element matrices [15], β is the propagation constant along the z axis shown in Fig. 1, and the $\{\phi\}$ is the eigenvector. The mode field distribution and β can be obtained by solving the Eq. (5).

3. SP-PBGF with an Anisotropic Lattice of Circular Air Holes

In this section, we investigate a novel structure of SP-PBGF with only circular air holes, which is based on the honeycomb photonic crystal lattice of air holes used in [13]. In [13], in order to obtain SP guidance, the sixfold rotational symmetry of a honeycomb PBGF is broken by introducing elliptical air holes into the core region. In general, introducing elliptical air holes requires sophisticated fabrication process. In this paper, in order to obtain SP guidance in the PBG type PCF, we introduce an anisotropic lattice of circular air holes into the core regions instead of using elliptical air holes. The cross-section of our SP-PBGF is shown in Fig. 1. This structure has large air holes around the core having an anisotropic air hole lattice structure, and these air holes are placed to suppress the higher order modes [13]. In this paper, the lattice pitch in the cladding is referred to as Λ and that in the core is referred to as Λ', as shown in Fig. 1. The air hole diameter in the cladding is assumed to be $d_1 = 0.55\Lambda$ and the diameter of large air holes in the 1st ring of cladding is assumed to be $d_2 = 1.2\Lambda$. The SP-PBGF consists of SiO_2 and air holes, and their refractive indices are $n_1 = 1.45$ and $n_2 = 1.0$, respectively. The lattice pitch in the core region is set to be $\Lambda' = \Lambda/4$. The FSM of the core has a birefringence due to the anisotropic lattice consisting of circular air holes.

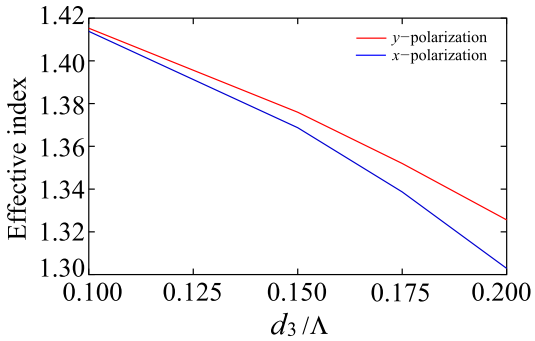

Fig. 3 Dispersion curves of FSM in the core. The effective indices of the x- and y-polarizations are shown with the red solid curve and blue solid curve, respectively.

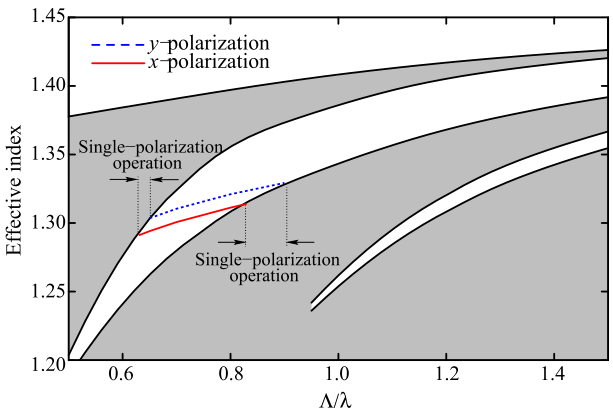

Fig. 4 PBG property and the dispersion curves of guided modes in the proposed PBGF. The white-colored areas represent PBG. The blue dashed and red solid curves show the x- and y-polarization guided modes, respectively.

In order to achieve the SP guidance with almost the same effective refractive index reported in [13], we investigate the effective index and birefringence of the core FSM and their air hole diameter dependences. Figure 3 shows the FSM index for each polarization mode with $d_3/\Lambda = 0.1 \sim 0.2$. In this analysis, the normalized operating wavelength is assumed to be $\lambda/\Lambda = 1.55$. From this result, we can see that the birefringence increases with d_3/Λ as we expect. In [13], the SP guidance is achieved around $n_{\text{eff}} = 1.35$. In order to achieve almost the same effective index of the SP guided mode, the air hole diameter in the core is set to be $d_3 = 0.7\Lambda' = 0.175\Lambda$. The dispersion curves of the PBG for the cladding region and the guided modes of SP-PBGF are shown in Fig. 4. The white regions represent the PBGs for the cladding region and the guided modes can be exist

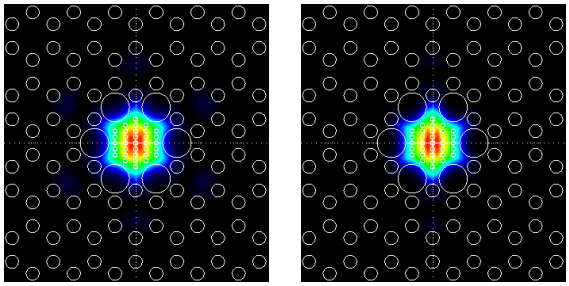

(a) x-SP mode (Λ/λ=0.63) (b) y-SP mode (Λ/λ=0.9)

Fig. 5 Mode field distribution for the SP mode of SP-PBGF.

Table 1 Overlap integrals between Gaussian field and mode field distribution.

	Eplitical air hole lattice	Anisotropic lattice
spot-size/Λ	2.2	2.24
overlap integral	~98%	~98%

only in this regions. The SP guidance can be achieved in the wavelength band where only the x- or y-polarized mode is cut off. In our proposed SP-PBGF, we can see that the x- and y-SP guidances can be achieved at the short and long-wavelength sides of the guided modes, respectively. Figure 5 shows the field distributions for the x- and y-SP modes at $\Lambda/\lambda = 0.63$ and 0.9, respectively. We can see that these mode field profiles are similar to a Gaussian profile. In order to evaluate the mode matching to a Gaussian field, we calculated the overlap integral between a Gaussian field and the mode field of the SP-PBGF shown in Fig. 5(b). Table 1 shows the maximum overlap integral value and the normalized spot-size of the corresponding Gaussian field. For comparison, those values for the SP-PBGF with elliptical air holes reported in [13] are also shown. In both cases, the overlap integrals can be up to 98% by adjusting the spot-size of the Gaussian field and good connection with conventional optical fibers and the other photonic crystal fibers may be expected. Figure 6 shows the chromatic dispersion originated from the complex air hole structure for the proposed SP-PBGF with $\Lambda = 1.32$ μm. Within the y-polarized SP wavelength band, reasonable wavelength dispersion of -10.6 to -3.2 ps/(km $\cdot$ nm) is obtained. On the other hand, within the x-polarized SP wavelength band, the chromatic dispersion is large.

Moreover, the wavelength bandwidth for the y-polarization is 124 nm when the center wavelength is assumed to be 1540 nm, and this wavelength bandwidth covers the (C+L) optical communication band. However, comparing with the SP band reported in [13], the SP band of our proposed SP-PBGF is narrow. This is because, the birefringence of our anisotropic lattice consisting of circular air holes is smaller than that of the elliptical air hole lattice. In addition, the effective indices of the guided modes are decreased from that of the FSM by the strong confinement of light in the core region. Therefore, the SP bandwidth becomes narrower than that reported in [13].

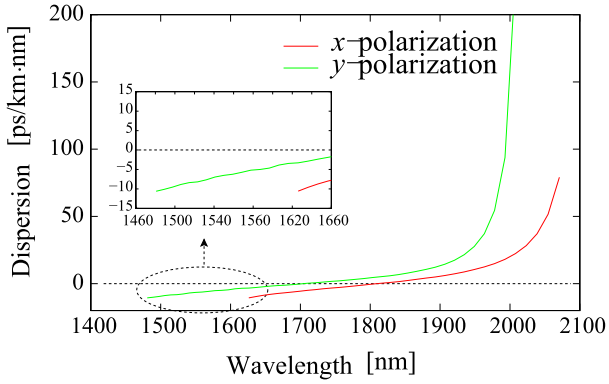

Fig. 6 Chromatic dispersion property in the proposed PBGF by setting $\Lambda = 1.32$ μm. The red and green solid curves show the chromatic dispersion of the x- and y-polarization, respectively.

4. Diameter and Lattice Pitch Dependences of SP Bandwidth

Though the PBGF shown in the previous section can realize the SP guidance, the SP bandwidth is narrower than that of the PBGF using an elliptical air hole lattice [13]. In this section, in order to obtain a wider SP band, we investigate the air hole diameter and lattice pitch dependences of the SP bandwidth and optimize the structural parameters of our SP-PBGF.

The wider SP band can be achieved by shifting the operating wavelength to the shorter (higher frequency) side. It is because the increasing rate of the PBG band edge is smaller at shorter wavelengths and the cut off wavelength difference between the x- and y-polarizations becomes larger for the same birefringence. The structural parameters of our PBGF need to be redesigned to make the operating wavelength shorter. Another strategy to get a wider SP bandwidth is to increase the birefringence. The larger birefringence leads to the larger cutoff wavelength difference between the two orthogonal polarizations.

In order to enlarge the polarization birefringence, first, we investigate the air hole diameter dependence of the bandwidth and birefringence. The air hole diameter in the core is set to be $d_3/\Lambda' = 0.6,\ 0.7$ and 0.8. The lattice pitch in the core region and the other structural parameters are set as the same values in the previous section. Figure 7 shows the air hole diameter dependence for the dispersion curves of the guided modes with $d_3/\Lambda' = 0.6,\ 0.7$ and 0.8. Table 2 shows the birefringence of FSM and the SP bandwidth estimated from Fig. 7. From these results, though the effective indices of the guided modes can be increased by setting d_3 smaller, the birefringence is getting smaller as d_3 decreases. Therefore, this strategy dose not seem to be quite effective to obtain a wider SP band.

After that, we investigate a lattice pitch Λ' dependence of the birefringence. In order to design the PBGF with a high birefringence, we investigate the lattice pitch dependence of the birefringence for the core FSM. Figure 8 shows

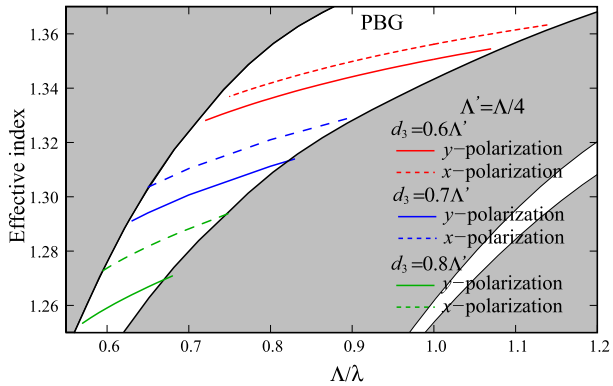

Fig. 7 Air hole diameter dependence for the dispersion curves of guided modes. the dashed and solid curves indicate the x- and y-polarizations, respectively. The red, blue and green curves correspond to $d_3/\Lambda' = 0.6$, 0.7 and 0.8, respectively.

Table 2 Birefringence and SP bandwidth shown in Fig. 7.

	d_3/Λ'		
	0.6	0.7	0.8
Birefringence	~0.005	~0.009	~0.014
SP Bandwidth	0.07	0.07	0.07

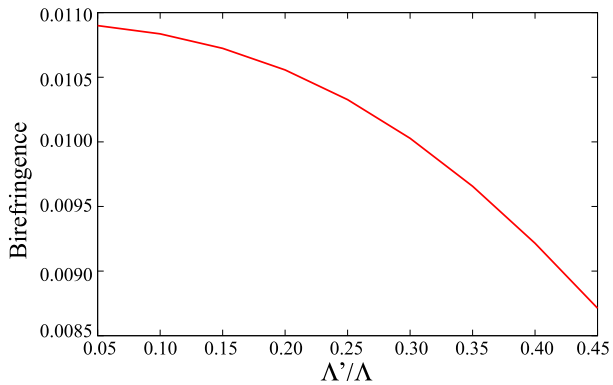

Fig. 8 Core lattice pitch dependence of the birefringence for the core FSM.

the lattice pitch Λ' dependence of the birefringence. Here, the normalized frequency is set to be $\Lambda/\lambda = 1.0$, the hole size of the core is $d_3/\Lambda' = 0.7$, and the lattice pitch of the core is considered from $\Lambda' = 0.05\Lambda$ to 0.45Λ. The other structural parameters are set as the same value as mentioned above. We can see that a higher birefringence is realized by setting the lattice pitch in the core smaller, and the SP guidance is expected to be achieved in the wider band. Next, we investigate the core lattice pitch dependence of birefringence for the SP-PBGF. The lattice pitch in the core is set to be $\Lambda' = \Lambda/6$, $\Lambda/4$ and $\Lambda/2.5$, and the other structural parameters are set as the same values as mentioned above. The relationship between the birefringence of SP-PBGF and the core lattice pitch Λ' is shown in Fig. 9. Figures 10(a),10(b), and 10(c) show the field distributions of the SP modes of SP-PBGFs with $\Lambda' = \Lambda/6$, $\Lambda/4$ and $\Lambda/2.5$, respectively. From these figures, we can see that the higher birefringence

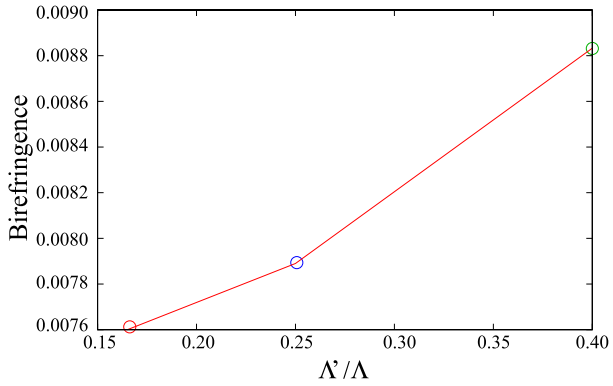

Fig. 9 Core lattice pitch dependence of the birefringence for the SP-PBGF.

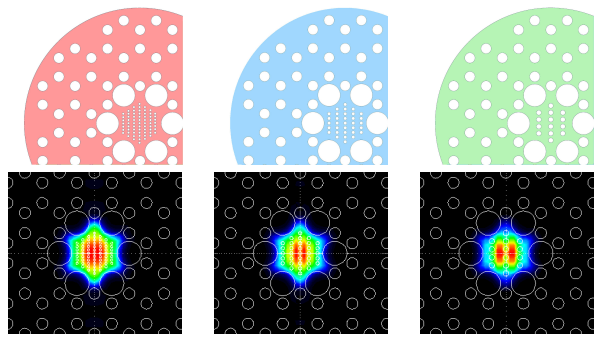

(a) $\Lambda' = \Lambda/6$ (b) $\Lambda' = \Lambda/4$ (c) $\Lambda' = \Lambda/2.5$

Fig. 10 Lattice pitch dependence for mode field distribution of the guided mode in the core (y-SP guided mode).

is obtained when the core lattice pitch Λ' is larger. This result seems to conflict with the result for FSM. However, in the case of waveguide modes, the smaller lattice pitch in the core region leads to an weaker light confinement in the anisotropic core region, which causes to reduce the modal birefringence. Therefore, we can see that, in this situation, the larger core lattice pitch Λ' is favorable to enlarge the modal birefringence.

5. Broaden the SP Bandwidth of SP-PBGF

In this section, based on the above discussion, we design the SP-PBGF with a wider SP band comparing to that discussed in Sect. 2. The core lattice pitch is selected to be $\Lambda' = \Lambda/2$, air hole diameter is $d_3 = 0.6\Lambda'(= 0.3\Lambda)$ or $0.66\Lambda'(= 0.33\Lambda)$, and the other structural parameters are set as the same values in the previous section. The dispersion properties of the PBG for the cladding region and the guided modes of SP-PBGF are shown in Fig. 11. From this figure, the effective indices of the guided modes are larger than those shown in Fig. 4 and the cutoff wavelength for each polarized mode is shifted to the shorter wavelength side comparing to that discussed in Fig. 4. Though the birefringence itself is smaller than that shown in Sect. 2, the difference of cutoff wavelength between the x- and y-polarizations is larger. Therefore, we can see that a wider SP bandwidth

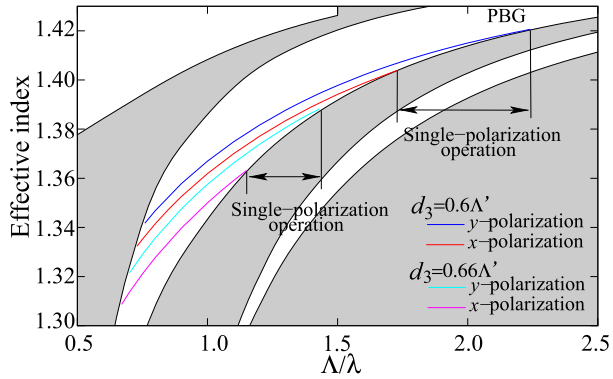

Fig. 11 Dispersion curves of SP-PBGF with a broaden SP bandwidth with Λ′=Λ/2. The blue and red solid curves show the dispersion curve with $d_3 = 0.6\Lambda'$, and the cyan and magenta solid curves show the dispersion curves with $d_3 = 0.66\Lambda'$.

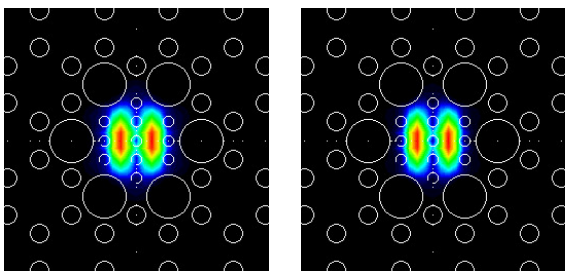

(a) y-SP mode (Λ/λ=1.75) (b) y-SP mode (Λ/λ=2.24)

Fig. 12 Mode field distribution of guided mode for SP-PBGF with $d_3 = 0.6\Lambda'$.

is realized. The mode field distribution of the SP-PBGF, whose hole size in the core is $d_3 = 0.6\Lambda'$, is shown in Fig. 12. We can see that only the y-polarized guided mode is supported and the SP guidance is achieved.

When the air hole diameter in the core is selected to be $d_3 = 0.6\Lambda'$ and the lattice pitch is set to be $\Lambda = 2.89\ \mu$m, the normalized frequency bandwidth is 0.51 that corresponds to a wavelength bandwidth of 388 nm and a center wavelength of 1495 nm. Therefore, this SP-PBGF can be used in the wide wavelength band covering the E-band to U-band. On the other hand, when the air hole diameter in the core is $d_3 = 0.66\Lambda'$ and the lattice pitch is $\Lambda = 1.88\ \mu$m, the normalized frequency bandwidth is 0.29, the wavelength bandwidth of 361 nm, and the center wavelength is 1494 nm. On this condition, this SP-PBGF has the almost same wavelength bandwidth as the structure with $d_3 = 0.6\Lambda'$. In these results, our proposed SP-PBGF with the optimized structural parameters can realize the SP guidance in an ultra wide wavelength band.

The propagation loss of PCF with a lot of air holes in the core region seems to be higher than that of conventional SMF due to the scattering loss caused by the surface roughness between air and silica. In order to estimate the scattering effect, we calculate the factor F reported in [16]. An estimated F value is $F = 0.25\ \mu\text{m}^{-1}$ for our proposed SP-PBGF with $d_3 = 0.6\Lambda'(= 0.3\Lambda)$ at the wavelength of

Table 3 Overlap integrals between Gaussian field and mode profile shown in Fig. 12.

	Fig. 12(a)	Fig. 12(b)
spot-size/Λ	1.73	1.7
overlap integral	~91%	~87%

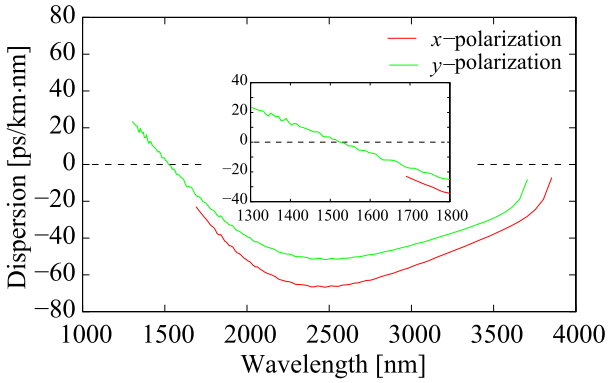

Fig. 13 Chromatic dispersion property in the proposed PBGF with $\Lambda = 2.89\ \mu$m and $d_3 = 0.6\Lambda' = 0.3\Lambda$. The red and green solid curves show the chromatic dispersion of the x- and y-polarization, respectively.

1.55 μm ($\Lambda = 2.89\ \mu$m). The F value and corresponding scattering loss reported in [16] are 0.0174 μm^{-1} and 3.5 dB/km, respectively. Comparing with the value in [16], the estimated F value of our proposed SP-PBGF is about 14 times larger and the corresponding scattering loss may be up to 50 dB/km. Table 3 shows the mode matching to the Gaussian field and the corresponding normalized spot-size. The overlap integrals of Figs. 12(a) and (b) with the Gaussian field can be up to 91% and 87% at the optimal normalized spot-size, respectively. The coupling efficiency to the conventional fibers is not so high for the butt coupling. In the directional coupler type devices from other types of fibers to this SP-PBGF, such as the polarization splitter in [17], the coupling efficiency may be improved. The structural design to improve coupling efficiency is one of our next issue. Figure 13 shows the chromatic dispersion of the proposed SP-PBGF with $\Lambda = 2.89\ \mu$m. The chromatic dispersion is relatively large in the longer wavelength band. However, about ±17 ps/(km · nm) is obtained in the SP wavelength range of 1363 ~ 1710 nm. The design to suppress the chromatic dispersion in this type of PBGF is also one of our next issue.

In the above discussion, the air hole diameter is expressed in a normalized scale. The actual hole size depends on the lattice pitch. Comparing with the SP-PBGFs discussed above, the former SP-PBGF with $\Lambda = 2.89\ \mu$m has a larger lattice pitch and a larger air hole size of $d_3/\Lambda' = 0.3\Lambda = 0.867\ \mu$m. Considering an actual fabrication, fine structures with smaller air holes require high-precision fabrication processes. That means the latter structure has an advantage in the actual fabrication.

6. Conclusion

In this paper, we proposed a novel SP-PBGF and designed

the structural parameters to achieve a wider SP bandwidth. Our proposed SP-PBGF can achieve wide band operation covering the E- to U- communication band, by selecting the optimal structural parameters, *i.e.*, the core lattice pitch and air hole diameter. However, the mode field profile is significantly different from those of standard SMFs. Therefore in future work, we will investigate the structure of SP-PBGF with an anisotropic air hole lattice to obtain a Gaussian like mode field distribution.

References

[1] J.C. Knight, T.A. Birks, P.St.J. Russell, and D.M. Atkin, "All-silica single-mode optical fiber with photonic crystal cladding," Opt. Lett., vol.21, no.19, pp.1547–1549, Oct. 1996.
[2] A.R. Bhagwat and A.L. Gaeta, "Nonlinear optics in hollow-core photonic bandgap fibers," Opt. Lett., vol.16, no.7, pp.5035–5047, March 2008.
[3] T.A. Birks, J.C. Knight, and P.St.J. Russell, "Endlessly single-mode photonic crystal fiber," Opt. Lett., vol.22, no.13, pp.961–963, July 1997.
[4] J. Broeng, D. Mogilevstev, E. Barkou, and A. Bjarklev, "Photonic crystal fibers: a new class of optical waveguides," Opt. Fiber. Technol., vol.5, pp.305–330, 1999.
[5] K. Saitoh and M. Koshiba, "Single-polarization single-mode photonic crystal fibers," IEEE Photon. Technol. Lett., vol.15, no.10, pp.1348–1386, Oct. 2003.
[6] H. Kubota, S. Kawanishi, S. Koyanagi, M. Tanaka, and S. Yamaguchi, "Absolutely single polarization photonic crystal fiber," IEEE Photon. Technol. Lett., vol.16, no.1, pp.182–184, Jan. 2004.
[7] J.R. Folkenberg, M.D. Nielsen, and C. Jakobsen, "Broadband single-polarization photonic crystal fiber," Opt. Lett., vol.30, no.12, pp.1446–1448, June 2005.
[8] J. Ju, W. Jin, and M.S. Demokan, "Design of single-polarization single-mode photonic crystal fiber at 1.30 and 1.55 μm," J. Lightw. Technol., vol.24, no.2, pp.825–830, Feb. 2006.
[9] M. Szpulaka, T. Martynkiena, J. Olszewskia, W. Urbanczyka, T.Nasilowskib, F. Berghmansb, and H. Thienpont, "Single-polarization single-mode photonic band gap fiber," ACTA Phy. Pol. A, vol.111, no.2, pp.239–245, 2007.
[10] A. Ferrandoa and J.J. Miret, "Single-polarization single-mode intraband guidance in supersquare photonic crystals fibers," Appl. Phys. Lett., vol.78, no.21, pp.239–245, May 2001.
[11] D.J.J. Hu, P. Shum, C. Lu, X. Yu, G. Wang, and G. Ren "Holey fiber design for single-polarization single-mode guidance," Appl. Opt., vol.48, no.20, pp.4038–4043, June 2009.
[12] M. Eguchi and Y. Tsuji, "Single-mode single-polarization holey fiber using anisotropic fundamental space-filling mode," Opt. Lett., vol.32, no.15, pp.2112–2114, Aug. 2007.
[13] M. Eguchi and Y. Tsuji, "Single-polarization elliptical-hole lattice core photonic-bandgap fiber," J. Lightw. Technol., vol.31, no.1, pp.177–182, Jan. 2013.
[14] K. Ichikawa, Z. Zhang, Y. Tsuji, and M. Eguchi, "A single-polarization holey fiber with anisotropic lattice of circular air holes," J. Lightw. Technol., vol.33, no.18, pp.3866–3871, Sept. 2015.
[15] M. Koshiba and Y. Tsuji, "Curvilinear hybrid edge/nodal elements with triangular shape for guide-wave problems," J. Lightw. Technol., vol.18, pp.2–3, May 2000.
[16] E.N. Fokoua, F. Poletti and D.J. Richardson, "Analysis of light scattering from surface roughness in hollow-core photonic bandgap fibers," Opt. Express, vol.20, no.19, pp.20980–20989, Sept. 2012.
[17] Z. Zhang, Y. Tsuji, and M. Eguchi, "Study on crosstalk-free polarization splitter with elliptical-hole core circular-hole holey fibers," J. Lightw. Technol., vol.32, no.23, pp.3956–3962, Dec. 2014.

Kazuki Ichikawa received the B.S. degree in department of information and electrical engineering from Muroran Institute of technology, Muroran, Japan,in 2013. He is presently working toward the M.S, degree in Information and Electronic Engineering from Muroran Institute of Technology. Mr. Ichikawa is a student member of the Institute of Electronics, Information and Communication Engineers (IEICE) and a student member of the IEEE.

Zejun Zhang received the B.S. degree in department of electrical engineering from Xuchang University, Xuchang, Henan, China, in 2011, and he received the M.S. degree in division of information and electronic engineering from Muroran Institute of Technology, Muroran, Japan, in2014. Mr. Zhang is a student member of the Institute of Electronics, Information and Communication Engineers (IEICE), and a student member of the IEEE.

Yasuhide Tsuji received the B.S., M.S., and Ph.D. degrees in electronic engineering from Hokkaido University, Sapporo, Japan, in 1991, 1993, and 1996, respectively. In 1996, he joined the Department of Applied Electronic Engineering, Hokkaido Institute of Technology, Sapporo, Japan. From 1997 to 2004, he was an Associate Professor of Electronics and Information Engineering at Hokkaido University. From 2004 to 2011, he was an Associate Professor of Electrical and Electronic Engineering at Kitami Institute of Technology, Kitami, Japan. Since 2011, he has been a Professor of Information and Electronic Engineering at Muroran Institute of Technology, Muroran, Japan. He has been interested in wave electronics. Dr. Tsuji is a member of the Institute of Electronics, Information and Communication Engineers (IEICE), the Japan Society of Applied Physics, the Optical Society of America (OSA), and IEEE. In 1997 and 1999, he was awarded the Excellent Paper Award from IEICE. In 2000, he has received the Third Millennium Medal from IEEE.

Masashi Eguchi received the B.S. degree in electronic engineering from Kitami Institute of Technology, Kitami, in 1985 and the M.S. and Ph.D. degrees in electronic engineering from Hokkaido University, Sapporo, Japan, in 1987, 1991, respectively. He joined Sony Co., Ltd., in 1987. From 1991 to 1995, he was with the Department of Industrial Design, Sapporo School of the Arts, Sapporo, Japan. And from 1995 to 1998, he was an Associate Professor of Center for Multimedia Aided Education at Muroran Institute of Technology, Muroran, Japan. Since 1998, he has been an Associate Professor of the Faculty of Science Technology, Chitose Institute of Science and Technology, Chitose, Japan. He has been engaged in research on various optical fibers, dielectric waveguides, optical solitons, and applications of finite element method and other electromagnetic wave analysis methods. Dr. Eguchi is a Senior Member of the Optical Society of America (OSA) and a Member of the Institute of Electronics, Information and Communication Engineers (IEICE).